



Contents lists available at ScienceDirect

# Spectrochimica Acta Part A: Molecular and Biomolecular Spectroscopy

journal homepage: [www.elsevier.com/locate/saa](http://www.elsevier.com/locate/saa)

## Synthesis, growth, thermal and optical studies on third order nonlinear optical material (E)-2-{3-[2-(4-chlorophenyl) vinyl]-5,5-dimethylcyclohex-2-en-1-ylidene}malononitrile for optoelectronic application



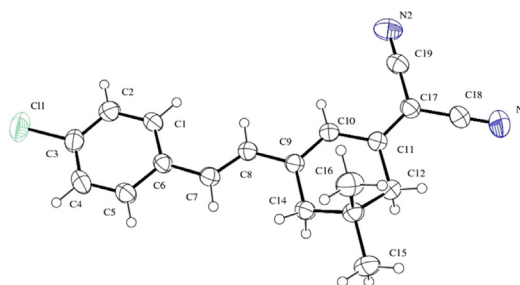
D. Bharath, S. Kalainathan\*

Centre for Crystal Growth, VIT University, Vellore 632014, Tamilnadu, India

### HIGHLIGHTS

- The Cl<sub>1</sub> material was synthesized and crystallized for optoelectronic application.
- The value of NLA ( $10^{-6}$  m/W) and NLRI ( $10^{-11}$  m<sup>2</sup>/W) were calculated by using Z-scan.
- The melting point and decomposition temperature of Cl<sub>1</sub> compound are 184.82 °C and 305.30 °C respectively.
- The crystal shows transparency from 610 nm onwards.
- The laser damage threshold of Cl<sub>1</sub> crystal is 431.84 MW/cm<sup>2</sup>.

### GRAPHICAL ABSTRACT

Molecular structure of Cl<sub>1</sub> compound.

### ARTICLE INFO

#### Article history:

Received 27 August 2013

Accepted 1 October 2013

Available online 12 October 2013

#### Keywords:

Organic compounds

Z-scan technique

Optical properties

Crystal growth

### ABSTRACT

A new polyene like organic molecule (E)-2-{3-[2-(4-chlorophenyl) vinyl]-5,5-dimethylcyclohex-2-en-1-ylidene}malononitrile (Cl<sub>1</sub>) was synthesized by knoevenagel condensation method. The Cl<sub>1</sub> Single crystals were successfully grown by the slow evaporation method at a constant temperature 35 °C. Single crystal XRD confirms the Cl<sub>1</sub> molecule belongs to monoclinic crystal system and space group *P2<sub>1</sub>/C* with *a* = 10.114, *b* = 11.127, *c* = 14.929 and *V* = 1668.9 and *Z* = 4. The grown Cl<sub>1</sub> crystals were subjected to FTIR and <sup>13</sup>C NMR studies to confirm the synthesized compound. The linear optical property of Cl<sub>1</sub> crystal has been studied using UV–Vis–NIR spectroscopy in the wavelength range 190 nm–1100 nm. The thermal properties of Cl<sub>1</sub> crystal were studied by using TG and DTA analysis. The refractive index of Cl<sub>1</sub> crystal has measured using Abbe's refractometer and found to be 1.648. The third order nonlinear optical property of Cl<sub>1</sub> crystal has been investigated using Z-scan technique with He–Ne laser. Photoluminescence (PL) spectrum of Cl<sub>1</sub> crystal was carried out using xenon lamp, which shows high intense emission peak at wavelength 614 nm. Laser optical damage threshold (LDT) of Cl<sub>1</sub> crystal has studied using Nd-YAG laser (10 Hz, 420 mJ, 1064 nm).

© 2013 Elsevier B.V. All rights reserved.

### Introduction

Revolutionizing the technological world, the opportunities for the use of organic materials in modern electric circuits based on the very high performance and long operational lifetime. There

has been an interest of industries and academic researches on organic conjugated materials for application like optical communications, light conversion, opto-electronics, flexible logic circuits and energy conversion [1]. The integral parts of fiber-optic transmission system are currently fabricated by rare earth doped semiconductor material. These components are costly to manufacture and restrict the technology for unique applications such as long distance telecommunications [2].

\* Corresponding author. Tel.: +91 416 2202350; fax: +91 0416 2243092.

E-mail address: [kalainathan@yahoo.com](mailto:kalainathan@yahoo.com) (S. Kalainathan).

The two photon absorption material is often a significant problem in the design of all optical switching devices because it occurs at the same order of nonlinearity as the intensity dependent refractive index ( $n_2$ ) (because these processes are proportional to the imaginary and real parts of  $\chi^3$  respectively) [3]. The identification of most favorable third-order NLO materials has become even more critical than second order materials. An interest to find the large third order organic nonlinear material in the near infra red region and to overcome the large nonlinear absorption loss, low nonlinear susceptibility, large linear absorption loss and lack of process ability for telecommunication bands. The most important organic molecules that absorb visible light can be classified into three categories such as polyenes, polymethines and porphyrines [4]. The candidate molecules polyene and cyanine dyes are one of the major ingredients of the optical response for large third order nonlinear optical application, and the large number of contribution is already reported in polyenes [5]. Organic Pi-conjugated materials can more easily tune by molecular design having strong optical nonlinearities and perform efficiently in all optical devices [6].

In this paper, we report the synthesis, growth on new Pi-conjugated organic 2-[3-[2-(4-chlorophenyl) vinyl]-5,5-dimethylcyclohex-2-en-1-ylidene]malononitrile crystal from dicyanomethylidene family. The structure of the compound has been confirmed by single crystal-XRD. FTIR has been recorded to analysis the functional group in molecular structure of synthesized Cl<sub>1</sub> compound and vibration analysis was studied. The third order susceptibility of organic material is calculated by Z-scan experiment using single Gaussian He–Ne laser beam. The nonlinear refractive index and nonlinear susceptibility was found to be of the order of  $10^{-11}$  m<sup>2</sup>/W and  $10^{-6}$  esu. A thermal study of Cl<sub>1</sub> compound was studied using TG and DTA analysis. The transparency range of crystal was studied using UV–Vis–IR absorption, and theoretically calculations are performed to calculate the optical constants. Laser damage threshold is necessary for fabrication of crystal and studied using Nd-YAG laser.

## Experimental section

### Material synthesis, crystal growth and morphology

The stoichiometric ratio 1:1 of the reactants malonodinitrile (10 mmol) and isophorone (10 mmol) were dissolved in solvent N-N-dimethylformamide in the presence of piperidine acetate as a catalyst, to synthesize 3,5-trimethylcyclohex-2-enylidene)malononitrile. The final product of the first step (3,5-trimethylcyclohex-2-enylidene)malononitrile (C<sub>12</sub>H<sub>14</sub>N<sub>2</sub>) was dissolved in chloroform (150 ml) with 4-chlorobenzaldehyde in equal molar ratio in the presence of piperidine acetate as a catalyst. The final product was recrystallized three times in glacial acetic acid. The purity of synthesized compound was improved by successive recrystallization process and filtration.

The orange coloured final product of 2-[3-[2-(4-chlorophenyl) vinyl]-5,5-dimethylcyclohex-2-en-1-ylidene]malononitrile (Cl<sub>1</sub>) (yield 60%) was synthesized. The structure of Cl<sub>1</sub> compound is shown in Fig. 1.

Cl<sub>1</sub> Single crystals have been grown by slow evaporation method. The most of the organic crystals are hygroscopic in nature, but the advantage of Cl<sub>1</sub> crystal is the lack of moisture sensitive. Cl<sub>1</sub> compound is insoluble in water, and it is highly soluble in polar solvents such as ethanol, acetonitrile, methanol and ethylmethyl ketone. The Cl<sub>1</sub> material was crystallized in different solvent, but it was found that ethyl methyl ketone has suitable medium for the growth of Cl<sub>1</sub> crystal. The dipole–dipole interactions between the Cl<sub>1</sub> molecule and solvent molecule are responsible for growth

of crystal and its morphology. The solubility of Cl<sub>1</sub> compound in ethyl methyl ketone was not too high compared with other solvents, 0.001 mole of the compound was dissolved of 25 ml of ethyl methylketone at room temperature. The saturation solution was allowed to evaporate slowly in beaker covered with aluminum foil with limited holes at a constant temperature 35 °C. The maximum size of brown colored Cl<sub>1</sub> crystals ( $12 \times 2 \times 1$  mm<sup>3</sup>) was harvested after the period of 10 days as shown in Fig. 2a.

The morphology of Cl<sub>1</sub> crystal has been generated from WINX-MORP software [7,8]. Crystal morphologies are predicted from single crystal *hkl* reflection data (CIF format). CIF data has given as input in the WINXMORP software, to predict the morphology of Cl<sub>1</sub> crystal. The morphology of Cl<sub>1</sub> crystal is growing along *b*-axis. The morphology of the crystal was shown in Fig. 2b.

## Characterization for compound confirmation

### Single crystal XRD and crystal packing structure

The crystallographic structure of Cl<sub>1</sub> crystal ( $0.35 \times 0.30 \times 0.25$  mm<sup>3</sup>) has been measured by single crystal XRD Bruker kappa apex-II diffractometer (Enraf Nonius CAD<sub>4</sub>-MV<sub>31</sub>). The Cl<sub>1</sub> crystal structure belongs to the monoclinic space group *P2<sub>1</sub>/C* (point group, *Z* = 4) is shown in Fig. 3. The strong coulomb forces binded a dicyanomethylidene acceptor and chlorobenzene donor in Pi-conjugated hydrogen bond. The unit cell of lattice parameters is *a* = 10.114(5), *b* = 11.127(5), *c* = 14.929(5) and *V* = 1668.9(12). In molecular packing as shown in Fig. 4, intermolecular interaction is between the hydrogen of the chlorobenzene electron donor group and one of the nitrogen of the nitrile electron acceptor group N<sub>2</sub>–H<sub>16</sub>A and N<sub>1</sub>–H<sub>4</sub>.

### Powder XRD

The powder XRD pattern of Cl<sub>1</sub> crystal is shown in Fig. 5. The well defined crystalline peaks at specific  $2\theta$  angles were obtained from powder form of Cl<sub>1</sub> crystal. The reflections (*hkl*) were indexed with corresponding crystalline peaks by using powderX program.

### FTIR

Fourier transform infrared spectroscopy has been recorded to analysis the functional group of synthesized Cl<sub>1</sub> compound and, it is shown in Fig. 6. In the wavelength range of 400–4000 cm<sup>-1</sup> was recorded using the instrument IR Affinity-1 (shimadzu) The weak stretching mode of –C–H– aldehyde is at 2929.87, 2825.72 cm<sup>-1</sup> and near to overlapping Fermi doublet. The methyl group –C–H– symmetric bending is observed at 1390.68 and 1371.39 cm<sup>-1</sup>. The strong symmetry stretching of –C–N– is assigned at 2289.50, 2222, 1531.48, 1180.44, 1155.38 cm<sup>-1</sup>. The aromatic –C=C– medium stretching in the benzene ring vibrations are at 1588.13 and 1487.12 cm<sup>-1</sup> and –C–C– bending at 1199.72 cm<sup>-1</sup>. The delocalized Pi–Pi bond of Cl<sub>1</sub> molecule shows strong =C–H– stretching at 1087.85 and 1006.84 cm<sup>-1</sup>. The strong symmetry stretching of nitrogen bonds is at 1338.60 and 1319.31 cm<sup>-1</sup>. –C–H– out of plane stretching vibrations are at 960.56, 941.26, 850.61 cm<sup>-1</sup> and –C–H– out of plane bending are at 761.88, 704.02 cm<sup>-1</sup>. The strong stretching of Chlorine atom in the molecule is at 542 cm<sup>-1</sup> [9]. The vibration analysis of Cl<sub>1</sub> crystallized material is shown in Table 1.

### <sup>13</sup>C Nuclear magnetic resonance

<sup>13</sup>C Nuclear magnetic resonance spectrum of Cl<sub>1</sub> has been recorded using dimethylsulfoxide (DMSO) as solvent on a Bruker

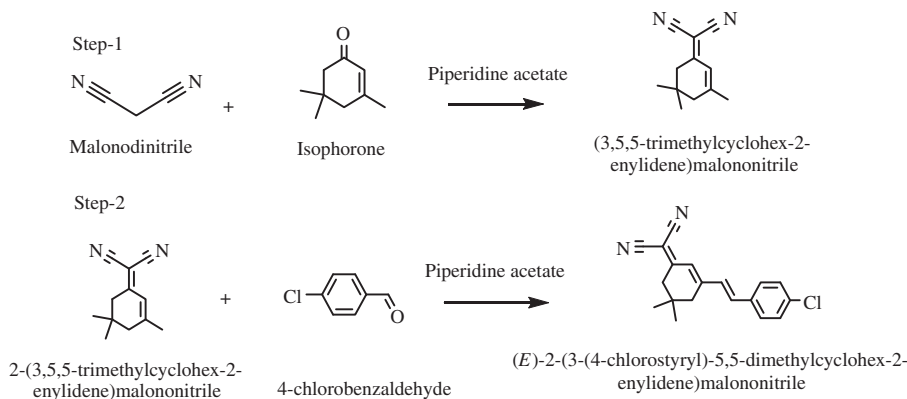


Fig. 1. Synthesis process of Cl<sub>1</sub> compound.

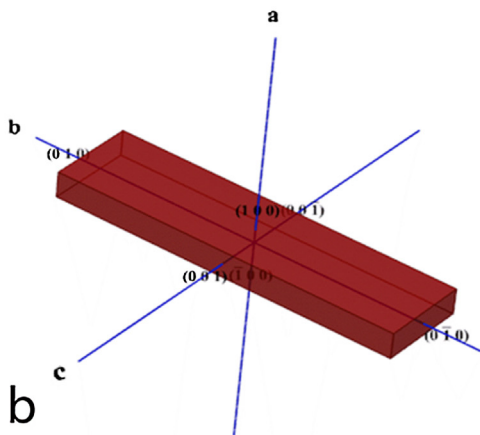
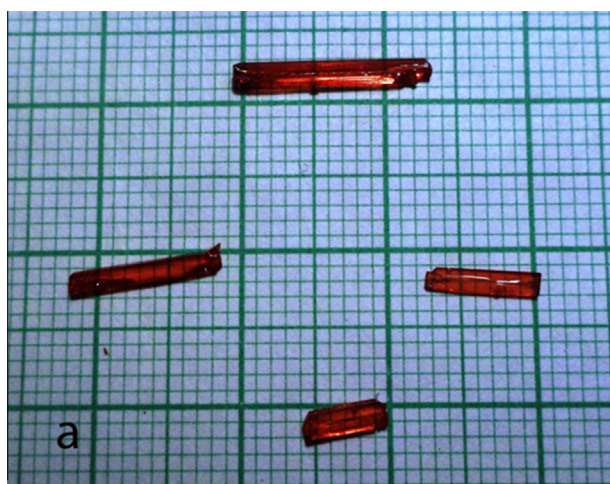


Fig. 2. (a) Cl<sub>1</sub> crystal grown in ethylmethyl ketone. (b) Morphology of grown Cl<sub>1</sub> crystal.

spectra instrument opening at 400 MHz, and it is shown in Fig. 7. <sup>13</sup>C NMR (DMSO, 400 MHz):  $\delta$ , 170.29, 155.44, 135.95, 133.92, 130.32, 129.41, 128.94, 123.24, 113.76, 112.94, 76.86, 48.59, 42.28, 38.14, 31.67 and 27.42 ppm. The aromatic carbon peaks are observed at 170.29, 155.44, 135.95, 133.92, 130.32, 129.41, 128.94, 123.24 ppm. The carbons in Pi–Pi bond are observed at 113.76 and 112.94. The cyano carbons shows peak at 76.86. The aliphatic carbons are observed at 48.59, 42.28, 38.14, 31.67 and 27.42 ppm. The number of carbons in Cl<sub>1</sub> molecule are matching with carbon peaks at <sup>13</sup>C NMR. The number of carbons in molecular

structure of Cl<sub>1</sub> compound is confirmed by <sup>13</sup>C nuclear magnetic resonance (NMR) spectral data.

### Thermal studies

The thermal stability of Cl<sub>1</sub> compound has been studied by thermo gravimetric (TG) and differential thermal analysis (DTA) as shown in Fig. 8. Cl<sub>1</sub> compound was analyzed in the temperature range 28–500 °C with a heating rate of 10 K/min in an inert nitrogen atmosphere. The melting point of Cl<sub>1</sub> compound was observed at 184.82 °C and that there is no loss of weight in the thermo gravimetric. It clearly indicates that there is no loss of a water molecule in Cl<sub>1</sub> molecule and it is free from water absorption. The endothermic peak at 305.30 °C in the DTA curve is due to the decomposition of compound. The decomposition temperature of closed locked polyene chromophores with the phenylhexatriene bridge is around 290 °C, reported by O.P. Kwon et al. There is a large temperature difference between melting point and decomposition temperature, and it is suitable for melt growth. It was noted that weight loss may be due to the decomposition or sublimation of the substance. The decomposition of Cl<sub>1</sub> compound, remaining residue left at 500 °C is 47%, it represents the decomposition occurs in 50% of compound.

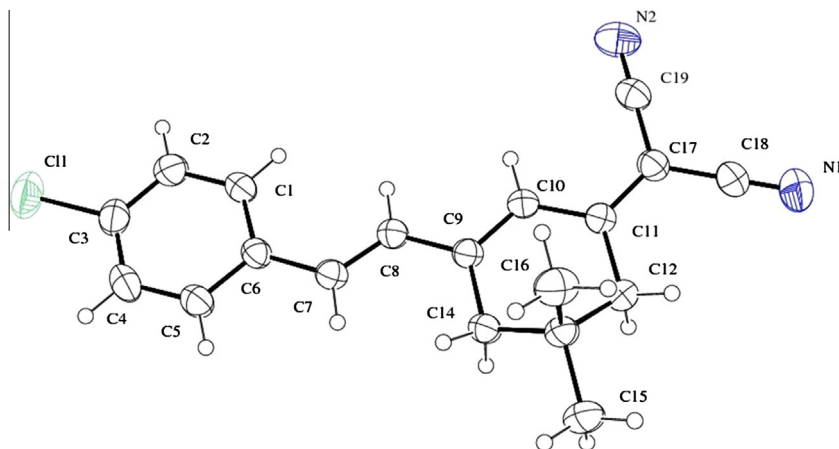
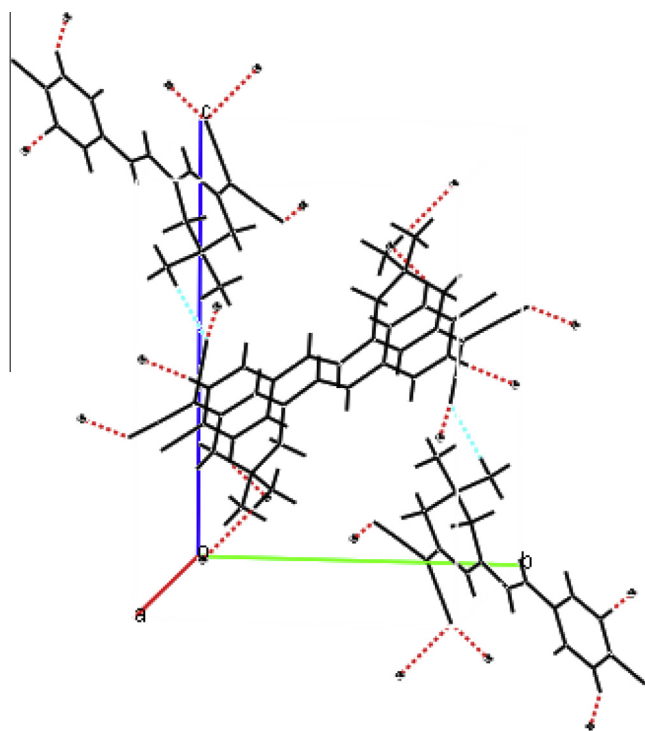
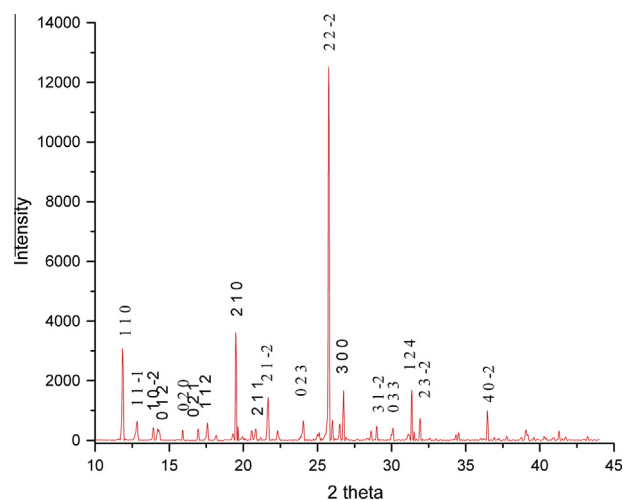
### Linear optical property

An interest of optical switching application has required finding the high third order NLO material, as well as large transmittance or low absorption in near infrared region. Fig. 9 shows the UV spectrum of Cl<sub>1</sub> crystal (1 mm thickness). The cutoff wavelength of Cl<sub>1</sub> crystal is at 610 nm, and it has very good optical transparency in near IR region. The optical absorption spectrum of Cl<sub>1</sub> crystal has been measured in the wavelength range 190–1100 nm by using double beam ultraviolet spectrophotometer (ELICO-SL218). The absorption or Pi–Pi\* transition at 380 nm is due to the presence of conjugate bond in Cl<sub>1</sub> molecule [10].

### Studies on optical band gap, optical conductivity, extinction coefficient

Absorption coefficient ( $\alpha$ ) of Cl<sub>1</sub> crystal has been calculated by using the equation  $\alpha = 2.303 \times \log (1/T)/d$ .

Where  $T$  is transmittance of crystal and  $d$  is thickness of the crystal. The absorption of Cl<sub>1</sub> crystal is low at higher wavelengths and high at lower wavelengths. The type of transition of an electron has studied from the plot, absorption coefficient vs wavelength. The four types of transitions are direct allowed transition ( $n = 1/2$ ), indirect allowed transition ( $n = 2$ ), direct forbidden

Fig. 3. Molecular structure of Cl<sub>1</sub> compound.Fig. 4. Molecular packing diagram of Cl<sub>1</sub> crystal.Fig. 5. Powder XRD pattern of Cl<sub>1</sub> compound.

transition ( $n = 3/2$ ) and indirect forbidden transition ( $n = 3$ ). As an indirect band gap crystal material, the optical band gap was calculated using the equation  $\alpha h\nu = A(Eg - h\nu)^n$ .

The graph is drawn between photon energy ( $h\nu$ ) versus  $(\alpha h\nu)^{1/2}$ . As shown in Fig. 10, the interpolation of the straight line from the absorption edge to photon energy axis ( $h\nu$ ) gives band gap. The Tauc's method has been used to measure the energy band gap of Cl<sub>1</sub> crystal, and it is 2.0029 eV [11].

The internal efficiency of optoelectronics devices are completely depending on the refractive index, absorption coefficient, optical conductivity, extinction coefficient and reflectance. It is important to determine the optical character of materials for suitable applications. Reflectance ( $R$ ) of Cl<sub>1</sub> crystal has been measured in terms of absorption coefficient by using the relation  $R = 1 \pm \text{Sqrt}(1 - \exp(-\alpha t) + \exp(\alpha t)) / 1 + \exp(-\alpha t)$ , where  $\alpha$  is absorption coefficient,  $t$  is thickness of crystal, and it is shown in Fig. 11. The refractive index ( $n$ ) was measured in terms of reflectance from the equation

$$n = -(R+1) \pm \text{Sqrt}(3R^2 + 10R - 3) / 2(R-1).$$

Optical conductivity of Cl<sub>1</sub> crystal is shown in Fig. 12 and it has calculated using the relation  $\sigma_{op} = \alpha \eta c / 4\pi$ . The increase in optical conductivity of material with respect to increase in photon energy shows the good optical response of the material. Extinction coefficient ( $K$ ) has been calculated using the relation  $\sigma_{op} = \alpha \eta c / 4\pi$  [12].

### Nonlinear optical property ( $\chi^3$ )

The precise measurements of sign and magnitude of third order nonlinear refractive index and absorption is carried out by using Z-scan method. It is an accurate method to determine both nonlinear absorption and nonlinear refraction of crystals, thin films and liquid solutions developed by Shakebahae et. al. This standard method has widely accepted by nonlinear optics community due to the simplicity of interpretation. The single Gaussian beam TEM<sub>00</sub> mode is allowed to pass through the sample along Z-axis. The focal length of a convex lens is completely depending on the Gaussian beam. The input intensity of He–Ne laser is 5 mW. The peak intensity of the incident laser beam was  $I_0 = 26.53 \text{ Mw/m}^2$ . The Gaussian beam was focused by a convex lens 30 mm to produce the beam waist  $\omega_0 = 12.26 \mu\text{m}$ . The essential criteria of Rayleigh length ( $Z_0 < L$ ) were found to be satisfied. The formula to measure the value is  $Z_0 = K\omega_0^2/2$ , where  $K$  is  $2\pi/\lambda$  and  $\omega_0$  is the radius of the laser beam at focal length.

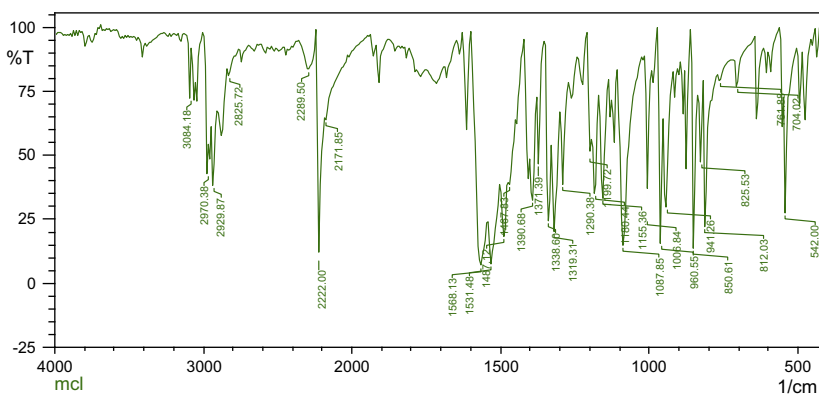


Fig. 6. FTIR pattern of Cl<sub>1</sub> compound.

Table 1

Observed FTIR bands of MOT2 compound and their assignments.

Observed wavenumbers (cm <sup>-1</sup> )	Assignments
3084.18m	—C—H aromatic stretching
2970.38m	C—H asymmetry bending in methyl group
2929.87w	C—H stretching in aldehyde
2825.72w	C—H stretching in aldehyde
2289.50m	—C≡N— stretching
2222.00s	—C≡N— stretching
1588.13s	—C=C— stretching
1531.48s	—C—N— stretching
1487.12s	—C=C— stretching of benzene ring
1390.68m	—C—H— bending in methyl group
1371.39m	—C—H— bending in methyl group
1338.60s	Symmetry stretching of nitrogen bonds
1319.31s	Symmetry stretching of nitrogen bonds
1199.72w	—C—C— bending
1180.44m	—C—N— stretching
1155.38m	—C—N— stretching
1087.85s	=C—H— stretching
1006.84s	=C—H— stretching
960.56s	—C—H— out of plane stretching
941.26s	—C—H— out of plane stretching
850.61s	—C—H out of plane stretching
825.53m	—C—H— bending
812.03s	Out of plane —C—H— stretching from disubstituted benzene ring
761.88w	—C—H— out of plane bending
704.02w	=C—H— out of plane bending
542.00s	—C—Cl— stretching

w – weak, s – strong, m – medium.

Z-scan technique is based on the conversion of amplitude distortion from phase distortion during the propagation of beam in sample. The experiment is scanning the sample through along the optical axis (z-axis) around the focal length of a convex lens. The sample can act as a thin lens of variable focal length. As the sample is brought closer to focus (at focal length), the irradiance of beam increases or decreases, depends on the material absorption and refractive index. The self defocusing effect increases the beam divergence, leading to beam broadening at the focal length. The saturation absorption enhances the peak and suppress the valley at the focal point of the optical path while the multiphoton absorption produces the reverse effect. This technique is useful to find the sign of nonlinear refractive index. The negative nonlinear refractive index of the sample shows transmittance peak followed by transmittance valley, similarly the positive nonlinear refractive index shows the transmittance valley followed by transmittance peak. The coefficient of nonlinear absorption can be easily calculated from maximum or minimum transmittance curves.

The magnitude of third order NLO susceptibility can be calculated using the formula  $\chi^3 = [Re(\chi^3) + Im(\chi^3)]$ . The real part of third

order susceptibility can be defined as  $Re(\chi^3) = 10^{-4} \epsilon_0 C^2 n_0^2 n_2 / \Pi$  (cm<sup>2</sup>/W) and the imaginary part of third order susceptibility can be defined as  $Im(\chi^3) = 10^{-2} \epsilon_0 C^2 n_0^2 \lambda \beta / 4 \Pi^2$  (cm /W). The real part of susceptibility is directly proportional to the nonlinear refractive index, and imaginary part of susceptibility is directly proportional to nonlinear absorption. The nonlinear absorption and nonlinear refractive index of crystal has measured in open and closed aperture method respectively. In closed aperture method, on-axis phase shift is calculated from valley-peak transmittance shown in Fig. 13a. The equation of on-axis phase shift ( $\Delta\Phi$ ) is in terms of normalized transmittance can be defined as  $\Delta T p - v = 0.406(1-S)^{0.25} |\Delta\Phi|$ , where  $S$  is the aperture linear transmittance ( $S=0.15$ ) and is calculated using the relation  $S = 1 - \exp[-2r_0^2/w_0^2]$ . The third order nonlinear refractive index of crystal can be defined in terms of on-axis phase shift  $\Delta\Phi = n_2 K l o L_{eff}$ . In open aperture method, nonlinear absorption  $\beta$  can be estimated from the relation  $\beta = 2\sqrt{2} \times \Delta T / l o L_{eff}$ . He—Ne laser is allowed to pass through 100 axis of Cl<sub>1</sub> crystal. The saturation absorption of Cl<sub>1</sub> crystal in open aperture method is shown in Fig. 13b. In the Z-scan approximation, instantaneous response of

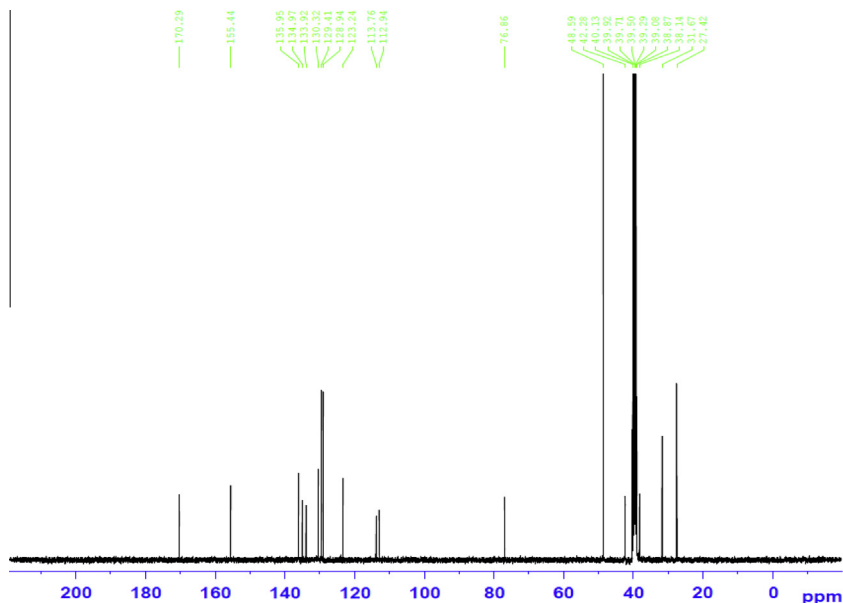


Fig. 7. <sup>13</sup>C nuclear magnetic resonance (NMR) spectral data for Cl<sub>1</sub> compound.

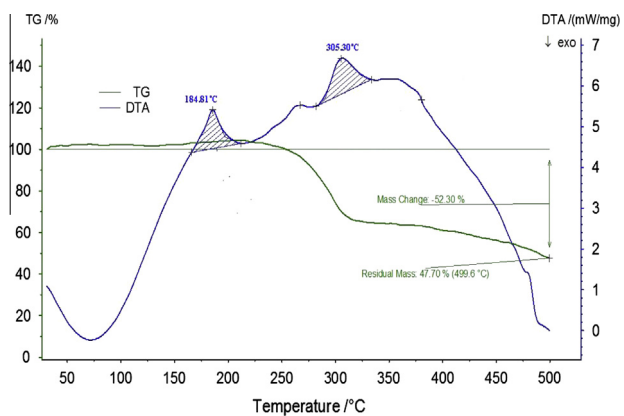


Fig. 8. TG/DTA studies of Cl<sub>1</sub> compound.

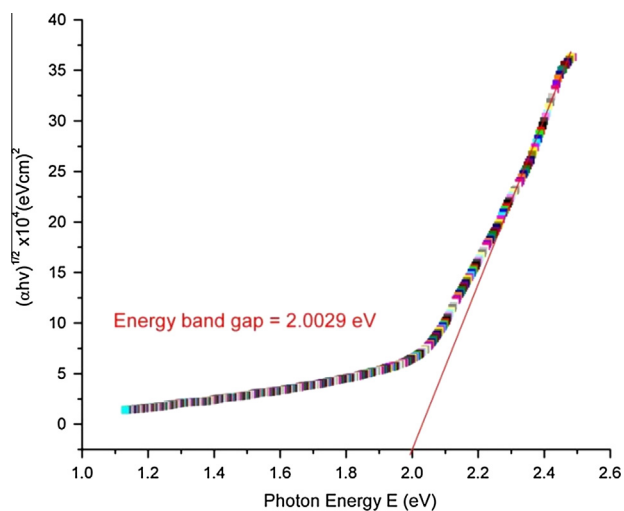


Fig. 10. Plot of  $(\alpha h\nu)^{1/2}$  vs photon energy for Cl<sub>1</sub> crystal.

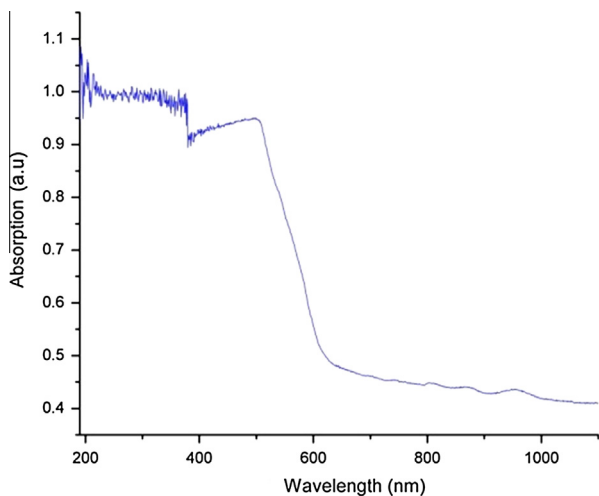


Fig. 9. Absorption spectrum of Cl<sub>1</sub> crystal.

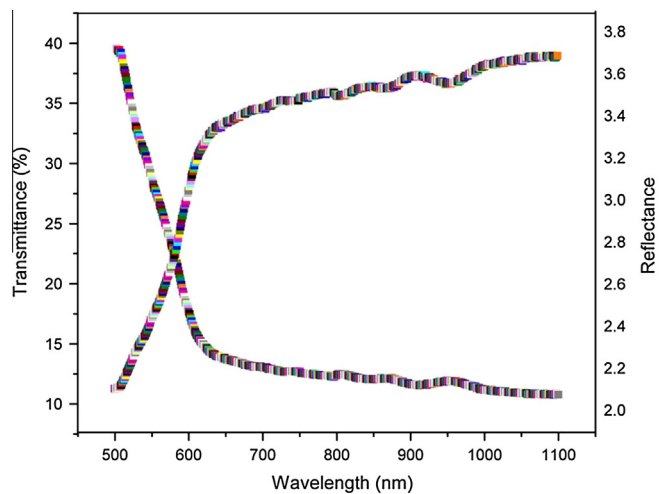


Fig. 11. Transmittance and reflectance spectrum of Cl<sub>1</sub> crystal.

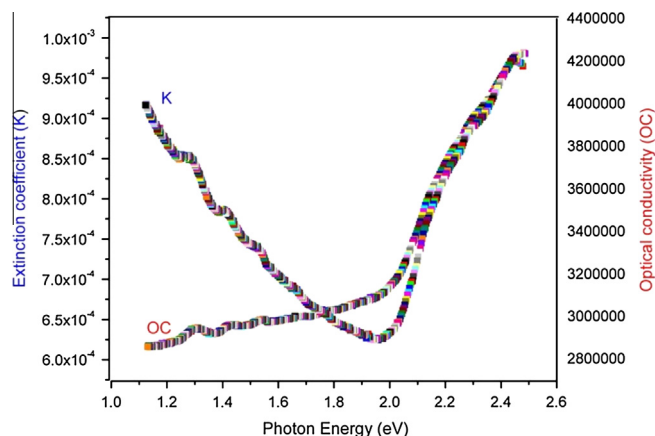


Fig. 12. Plot of optical conductivity and extinction coefficient of  $\text{Cl}_1$  crystal.

Table 2

Z-scan techniques measurement data.

Laser beam wavelength ( $\lambda$ )	633 nm
Focal length of lens	30 mm
Optical path length	75 cm
Beam radius of the aperture ( $w_a$ )	3.5 mm
Aperture radius ( $r_a$ )	1 mm
Sample thickness ( $L$ )	0.582 mm
Beam radius ( $W_o$ )	12.26 $\mu\text{m}$
Effective thickness ( $L_{\text{eff}}$ )	0.6535 mm
Linear absorption coefficient ( $\alpha$ )	0.9212
Linear transmittance ( $S$ )	0.15
Rayleigh length ( $Z_o$ )	2.44 mm
Intensity at focus ( $I_o$ )	26.47 $\text{Mw}/\text{m}^2$
Phase change ( $\Delta\Phi$ )	0.1063
Nonlinear refractive index ( $n_2$ )	$5.476 \times 10^{-11} \text{ m}^2/\text{W}$
Nonlinear absorption coefficient ( $\beta$ )	$-2.3539 \times 10^{-6} \text{ m}/\text{W}$
Real part of third order susceptibility [ $\text{Re}(\chi^3)$ ]	$1.1851 \times 10^{-6} \text{ esu}$
Imaginary part of third order susceptibility [ $\text{Im}(\chi^3)$ ]	$2.5313 \times 10^{-6} \text{ esu}$
Third order nonlinear susceptibility ( $\chi^3$ )	$2.7949 \times 10^{-6} \text{ esu}$

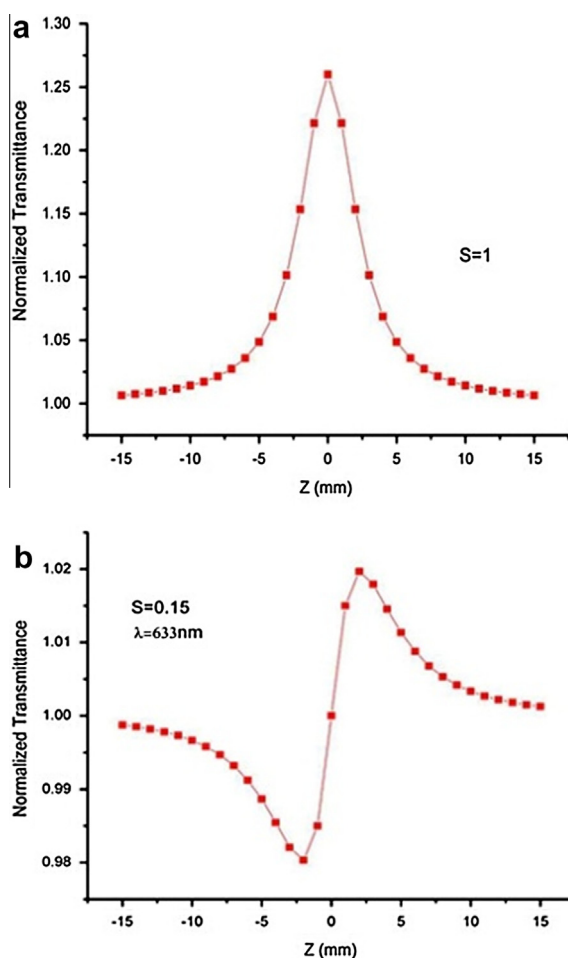


Fig. 13. (a) Negative saturation absorption of  $\text{Cl}_1$  crystal in open aperture. (b) Self focusing effect of  $\text{Cl}_1$  crystal in closed aperture.

refractive index and absorption coefficient at strong electromagnetic field is given by  $n = n_o + n_2 I$  and  $\alpha = \alpha_o + \beta I$ , where  $n_o$  and  $\alpha_o$  are linear optical property of refractive index and absorption coefficient,  $n_2$  and  $\beta$  are nonlinear optical property of nonlinear refractive index, and nonlinear absorption and  $I$  is the intensity of the laser beam.

To neglect the nonlinear absorption of closed aperture normalized transmittance ( $\Delta T_{CA}$ ) can be defined as  $\Delta T_{CA} = 1 - [4 \times \Delta\Phi / (x^2 + 1)(x^2 + 1)]$ , where  $x = z/z_o$ ,  $z_o$  is Rayleigh length. The condition

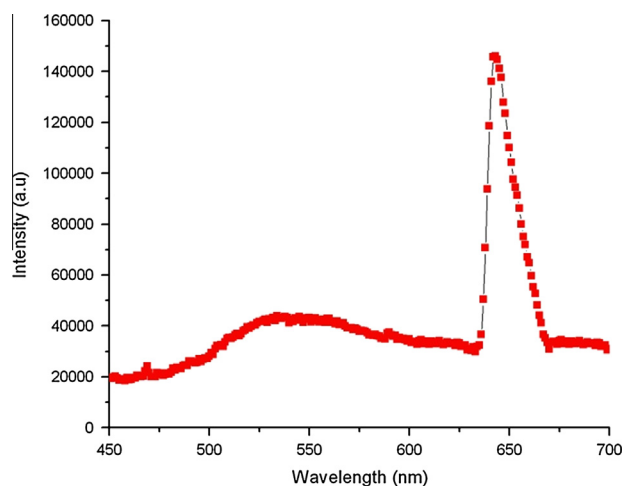


Fig. 14. Photoluminescence spectrum of  $\text{Cl}_1$  crystal.

for normalized transmittance for open aperture method is given by [For  $q_o(0) < 1$ , where  $q_o(0) = \beta I_o L_{\text{eff}} / (1 + (z^2/z_o^2))$ ] [13].

$$\Delta T_{OA}(Z, S = 1) = \sum_{m=0}^{\infty} [q_o(Z)]^m / (m + 1)^{3/2}$$

The negative nonlinear absorption has been observed in  $\text{Cl}_1$ , due to the saturation absorption of material. The calculated value of nonlinear absorption ( $\beta$ ) is  $2.3539 \times 10^{-6} \text{ m}/\text{W}$ . The change in transmittance (valley-peak) of  $\text{Cl}_1$  materials shows self focusing effect in closed aperture method. The calculated value of nonlinear refractive index of material is  $5.476 \times 10^{-11} \text{ m}^2/\text{W}$ . The third order nonlinear susceptibility ( $\chi^3$ ) of  $\text{Cl}_1$  crystal is  $2.7949 \times 10^{-6} \text{ esu}$ . The measurement details of Z-scan technique is shown in Table 2.

## Photoluminescence

The photoluminescence (PL) of  $\text{Cl}_1$  crystal has shown in Fig. 14, and it is recorded in the range of 450–700 nm. The high pressure 450 W Xenon lamp (John Yvon-spex spectrometer-FL3-11) was used to measure the excitation wavelength of PL spectrum. The high intensity of fluorescence spectrum at 642.5 nm is 146,280 a.u. The excitation wavelength of PL spectrum has given at 502 nm with a spectral resolution of 0.2 nm. The energy band gap of  $\text{Cl}_1$  crystal has calculated to be 2.032 eV, using the formula  $E_g = 1.24/\lambda \text{ eV}$ . Where  $h$ ,  $c$ ,  $e$  are constants and  $\lambda$  is the wavelength of fluorescence.

### Laser damage threshold (LDT)

The application of crystalline material is limited by one of the optical property, low laser damage threshold. The LDT of Cl<sub>1</sub> crystal has been measured by using Nd-YAG laser (420 mJ, 10 Hz). The focal length of a convex lens is 300 mm, placed between laser source and power meter (Coherent energy meter EPM-200). The diameter of the laser beam 1 mm at focal length is allowed to damage the surface of Cl<sub>1</sub> (5 × 2 × 1 mm<sup>3</sup>) crystal by varying the analog power supply of laser having nanosecond pulse duration. It is noted that 67.8 mJ of laser energy initiating the crack after 30 s on the surface of Cl<sub>1</sub> crystal (100 plane). Laser damage threshold of Cl<sub>1</sub> crystal is 431.847 MW/cm<sup>2</sup>, and it is calculated from the relation, Energy density = input energy/area (Gw/cm<sup>2</sup>).

### Conclusion

A promising organic material for optoelectronic application was synthesized, and single crystal (E)-2-[3-[2-(4-chlorophenyl) vinyl]-5,5-dimethylcyclo-hex-2-en-1-ylidene]malononitrile has been grown by slow evaporation method for optical switching application. The magnitude of nonlinear refractive index (10<sup>-11</sup> m<sup>2</sup>/W), nonlinear absorption (10<sup>-6</sup> m/W) and third order nonlinear susceptibility (10<sup>-6</sup> esu) has been studied using Z-scan technique. The melting point and decomposition temperature of Cl<sub>1</sub> compound are 184.82 °C and 305.30 °C respectively. The optical transmission study reveals the cutoff wavelength of Cl<sub>1</sub> crystal is 610 nm. The optical conductivity, optical band gap and extinction coefficient of Cl<sub>1</sub> crystal was studied from UV absorption spectrum.

PL spectrum exhibits red fluorescence emission. The laser damage threshold energy of Cl<sub>1</sub> crystal is 67.8 mJ, and the energy density is 431.847 MW/cm<sup>2</sup>. The spectroscopic characterization of FTIR, powder-XRD, single crystal XRD and proton NMR are studied.

### Acknowledgements

The authors thank the management of VIT University Vellore for proving the excellent research facilities. The author acknowledges Dr. U. Madhusoodanan, IGCAR for PL Studies and also the authors are very much thankful to SAIF, IIT madras for providing the single crystal XRD data.

### References

- [1] S.R. Forrest, Nature 428 (2004) 911.
- [2] S.A. Haque, J. Nelson, Science 327 (2010) 1466.
- [3] R.W. Boyd, Nonlinear Optics, third ed., Elsevier publications, 2011.
- [4] H.J. Kuhn, Chem. Phys. 17 (1949) 1198.
- [5] O.P. Kwon, B. Ruiz, A. Choubey, L. Mutter, A. Schneider, M. Jazbinsek, V. Gramlich, P. Gunter, Chem. Mater. 18 (2006) 4049.
- [6] J.M. Hales, J. Matichak, S. Barlow, S. Ohira, K. Yesudas, J.L. Bredas, J.W. Perry, S.R. Marder, Science 327 (2010) 1485.
- [7] W. Kaminsky, J. Appl. Cryst. 38 (2005) 566.
- [8] W. Kaminsky, J. Appl. Cryst. 40 (2007) 382.
- [9] P.S. Kalsi, Spectroscopy of Organic Compounds, sixth ed., New Age International Publisher, 2007.
- [10] S.G. Amridha, S. Kalainathan, J. Phys. Chem. Solids 72 (2011) 961.
- [11] C.A. Kumar, D. Kaur, R. Chandra, Opt. Mater. 29 (2007) 995.
- [12] D.D.O. Eya, A.J. Ekpunobi, C.E. Okeke, Acad. Open Internet J. 17 (2006) 13.
- [13] M. Sheik-bahae, A.A. Said, T. Wei, D.J. Hagan, E.W. Van styland, IEEE J. Quantum Electron. 26 (1990) 4.